Electronic Supplementary Material (ESI) for RSC Advances.

Supporting Information

Thermally-induced bilayered crystals in solution-processed polycrystalline thin film of phenylterthiophene-based monoalkyl smectic liquid crystals and its effect on FET mobility

Hao Wu, Hiroaki Iino, and Jun-ichi Hanna*

Imaging Science and Engineering Research Center, Tokyo Institute of Technology, J1-2, 4259 Nagatsuta, Midori-ku, Yokohama 226-8503, Japan.

*Corresponding author. E-mail: hanna@isl.titech.ac.jp

Table of Contents

1. Synthesis and Characterization

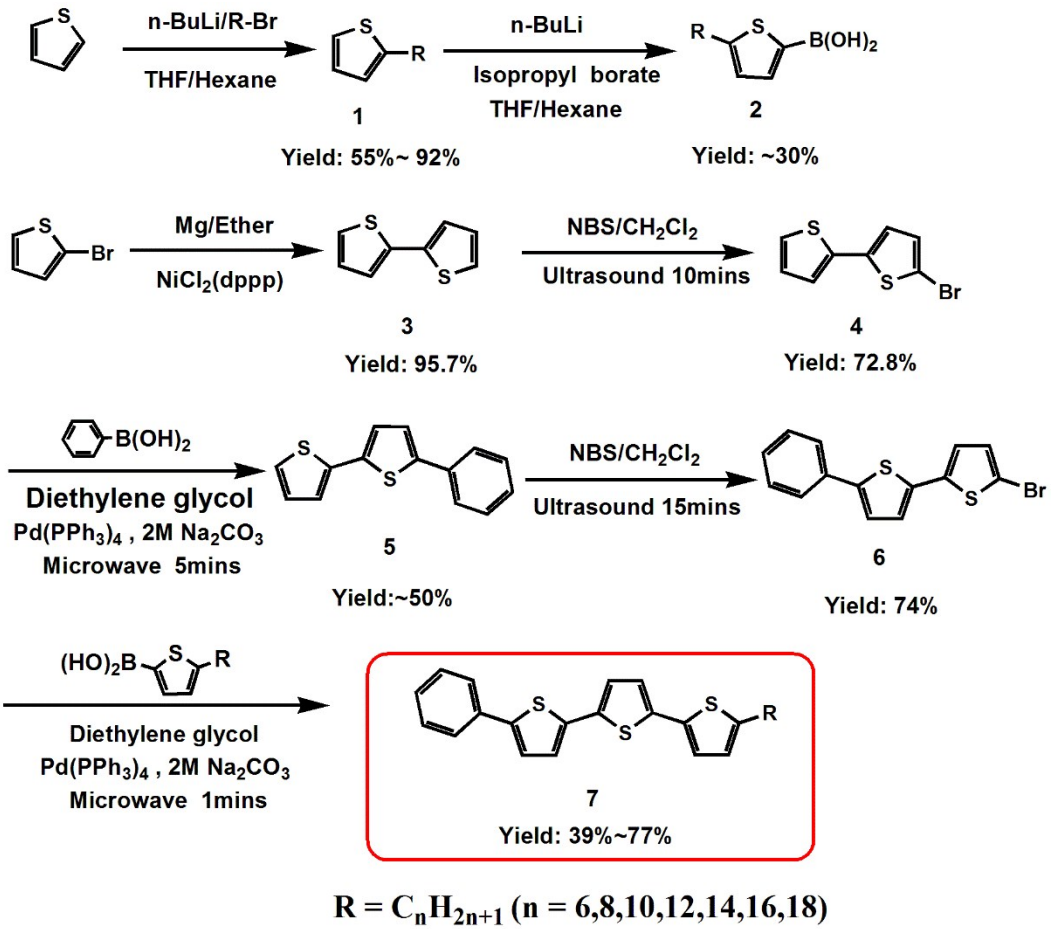

Scheme S1. Synthesis route of Ph-$(Tp)_3$-Cn

2-alkyl thiophene (1)

To a stirred solution of thiophene 2.02g (24mmol) in 30ml anhydrous THF, 15ml n-BuLi/hexane solution (1.6M, 24mmol) was added slowly at -78°C under argon. After stirring at -78°C for 15min, 23mmol n- alkyl bromides were added in one portion. Then the cooling source was removed, and left stirring overnight. Water was slowly added and the mixture was extracted with ethyl acetate. The organic layer was dried over Na_2SO_4, filtrated, and evaporated. The crude product was purified by column chromatography on silica gel (hexane) to give pure colorless oils in 55%~92% yields.

2-octadecyl thiophene (92%): ^{1}H-NMR ($CDCl_3$, 400 MHz): δ 7.09-7.11 (d-d, 1H), 6.90-6.92 (m, 1H), 6.77-6.78 (m, 1H), 2.80-2.83 (t, 2H), 1.63-1.71 (m, 2H), 1.26-1.37 (m, 30H), 0.86-0.90 (t, 3H).

2-hexadecyl thiophene (86%): ^{1}H-NMR ($CDCl_3$, 400 MHz): δ 7.09-7.11 (d-d, 1H), 6.90-6.92 (m, 1H), 6.77-6.78 (m, 1H), 2.79-2.83 (m, 2H), 1.63-1.69 (m, 2H), 1.26-1.37 (m, 26H), 0.86-0.90 (t, 3H).

2-tetradecyl thiophene (78%): ^{1}H-NMR ($CDCl_3$, 400 MHz): δ 7.09-7.11 (d-d, 1H), 6.90-6.92 (m, 1H), 6.77-6.78 (m, 1H), 2.79-2.83 (m, 2H), 1.63-1.71 (m, 2H), 1.26-1.37 (m, 22H), 0.86-0.90 (t, 3H).

2-dodecyl thiophene (79%): ^{1}H-NMR ($CDCl_3$, 400 MHz): δ 7.09-7.11 (d-d, 1H), 6.90-6.92 (m, 1H), 6.77-6.78 (m, 1H), 2.79-2.83 (m, 2H), 1.63-1.71 (m, 2H), 1.26-1.37 (m, 18H), 0.86-0.90 (t, 3H).

2-decyl thiophene (90%): ^{1}H-NMR ($CDCl_3$, 400 MHz): δ 7.09-7.10 (d-d, 1H), 6.89-6.92 (m, 1H), 6.76-6.78 (m, 1H), 2.79-2.83 (m, 2H), 1.63-1.71 (m, 2H), 1.26-1.44 (m, 14H), 0.86-0.90 (t, 3H).

2-octyl thiophene (69%): ^{1}H-NMR ($CDCl_3$, 400 MHz): δ 7.09-7.11 (d-d, 1H), 6.90-6.92 (m, 1H), 6.77-6.78 (m, 1H), 2.80-2.83 (t, 2H), 1.63-1.71 (m, 2H), 1.27-1.38 (m, 10H), 0.86-0.90 (t, 3H).

2-hexyl thiophene (55%): ^{1}H-NMR ($CDCl_3$, 400 MHz): δ 7.09-7.10 (d-d, 1H), 6.90-6.92 (m, 1H), 6.77-6.78 (m, 1H), 2.80-2.83 (t, 2H), 1.63-1.71 (m, 2H), 1.26-1.37 (m, 6H), 0.86-0.90 (t, 3H).

5-alkyl-2-thiopheneboronic acid (2)

To a stirred solution of 2-alkylthiophene (10mmol) in 12ml anhydrous THF, 6.8ml n-BuLi/hexane solution (1.6M, 11mmol) was added slowly at -78°C under argon. After stirring at -78°C for 15min, 2.8ml triisopropyl borate (12mmol) was added in one portion. Then the cooling source was removed, and left stirring overnight. 12ml 2M hydrochloric acid was slowly added and the mixture was extracted with toluene. The organic layer was dried over Na_2SO_4, filtrated, and evaporated. The crude product was purified by adding small amount of ether to precipitate white solid product in refrigerator in ~30% yields. The product was not stable and used in next step without further purification.

5-bromo-5'-phenyl-2,2'-bithiophene (6)

To a stirred solution of 5'-phenyl-2,2'-bithiophene (5) (5mmol) in 120ml CH_2Cl_2, NBS 0.98g (5.5mmol) was added slowly in one portion. After irradiated by ultrasound at room temperature for 15min, Na_2SO_3 solution was added. The mixture was extracted with CH_2Cl_2 and washed with water. The organic layer was dried over Na_2SO_4, filtrated, and evaporated. The crude product was purified by column chromatography on silica gel (cyclohexane), or recrystallized from ethanol to give pure white lamellar crystal in 74% yield. ^{1}H-NMR ($CDCl_3$, 400 MHz): δ 7.57-7.59 (m, 2H), 7.37-7.41 (m, 2H), 7.27-7.31 (m, 1H), 7.21-7.22 (d, 1H), 7.08-7.09 (d, 1H), 6.98-6.99 (d, 1H), 6.93-6.94 (d, 1H).

2. Mesomorphic behaviors

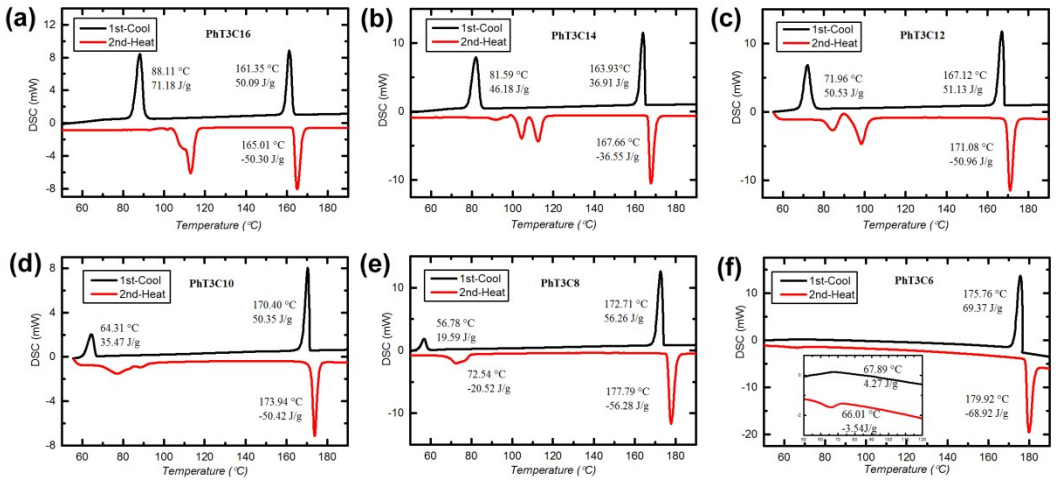

Fig. S1 DSC curves (10°C min^{-1}) of **Ph-(Tp)$_3$-Cn** (6, 8, 10, 12, 14, 16)

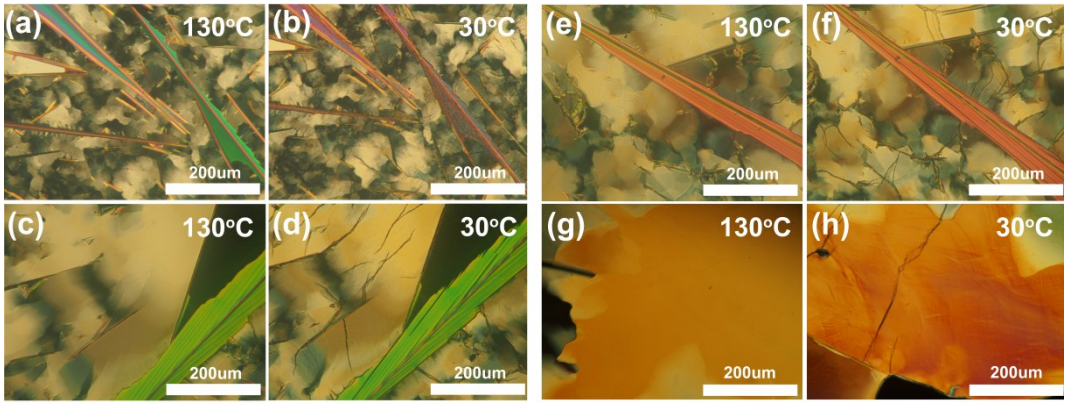

Fig. S2 POM textures of Ph-(Tp)$_3$-C16 at 130°C (a), at 30°C (b); Ph-(Tp)$_3$-C12 at 130°C (c), at 30°C (d); Ph-(Tp)$_3$-C10 at 130°C (e), at 30°C (f); Ph-(Tp)$_3$-C6 at 130°C (g), at 30°C (h).

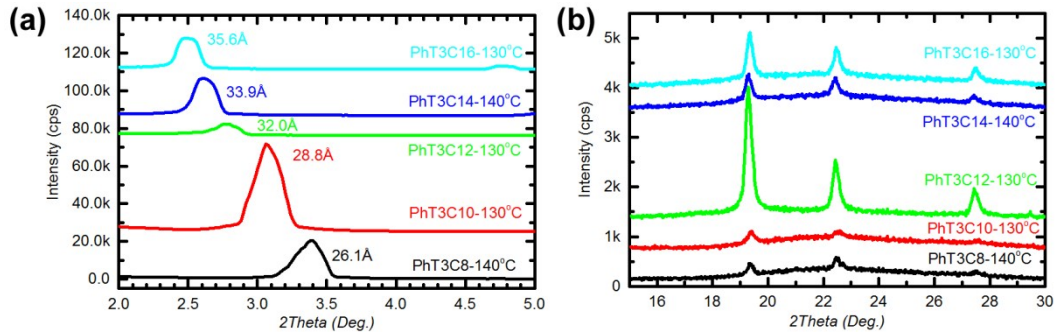

Fig. S3 Bulk film XRD patterns of Ph-(Tp)$_3$-Cn (8, 10, 12, 14, 16) on heating at SmE phase.

3. Bilayer structure formation of Ph-(Tp)$_3$-C18 in polycrystalline thin films under different TA temperature

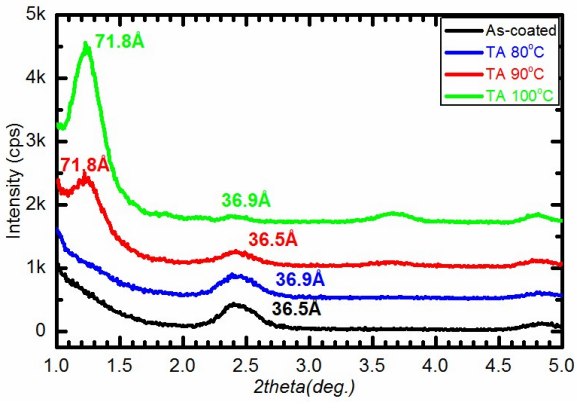

Fig. S4 Thin film XRD pattern of Ph-(Tp)$_3$-C18 before and after TA at different temperatures in the crystal state

4. Bilayer structure characterization

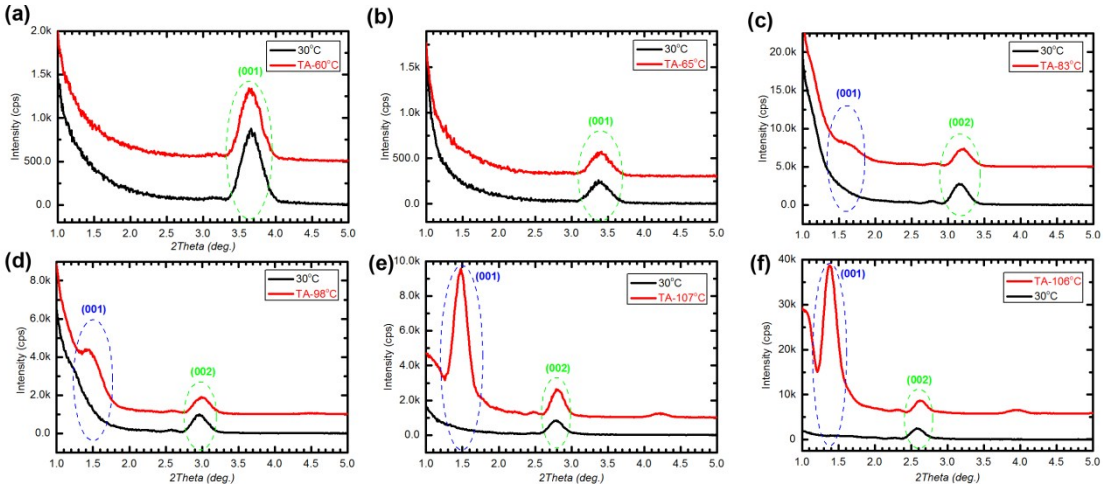

Fig. S5 Thin film XRD patterns of (a) Ph-(Tp)$_3$-C6, (b) Ph-(Tp)$_3$-C8 at Cr1 phase and TA at a temperature near the transition point of Cr to SmE; thin film XRD patterns of (c) Ph-(Tp)$_3$-C10, (d) Ph-(Tp)$_3$-C12, (e) Ph-(Tp)$_3$-C14, (f) Ph-(Tp)$_3$-C16 before and after TA at Cr2 phase.

5. DSC of Ph-(Tp)$_3$-C18 at 1°C min^{-1}

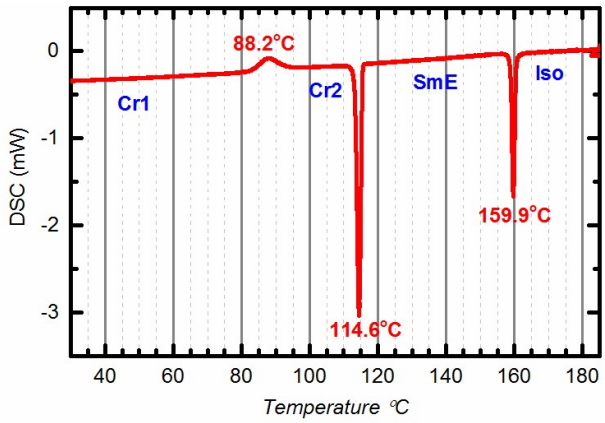

Fig. S6 DSC of Ph-$(Tp)_3$-C18 at 1°C min^{-1} on 2nd heating run (the sample was firstly heated to Iso and then quenched by liquid N_2)

6. OFETs properties

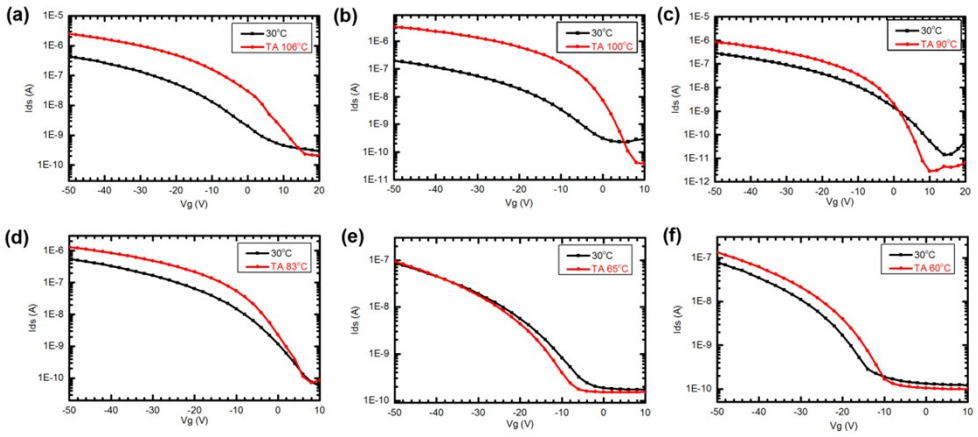

Fig. S7 Transfer characteristics of (a) Ph-$(Tp)_3$-C16, (b) Ph-$(Tp)_3$-C14, (c) Ph-$(Tp)_3$-C12, (d) Ph-$(Tp)_3$-C10 before and after TA at Cr2 phase; (e) Ph-$(Tp)_3$-C8, (f) Ph-$(Tp)_3$-C6 at Cr1 phase and TA at a temperature near the transition point of Cr to SmE (V_{ds} = -50V).

Table S1 Summary of OFET properties of Ph-$(Tp)_3$-Cn

Names	T [a]	μ($cm^2V^{-1}s^{-1}$) [b]	$R_{a/b}$ [c]	$I_{on/off}$	V_{th} (V)
Ph-$(Tp)_3$-C18 [d]	Cr1 state (30°C)	4.6×10^{-3}	21.3	1.6×10^{4}	0.4
	Cr2 state (TA 100°C)	9.6×10^{-2}		9.65×10^{5}	3.0
Ph-$(Tp)_3$-C16	Cr1 state (30°C)	6.2×10^{-3}	4.4	1.8×10^{3}	0
	Cr2 state (TA 106°C)	2.7×10^{-2}		3.1×10^{4}	8.3
Ph-$(Tp)_3$-C14 [d]	Cr1 state (30°C)	3.1×10^{-3}	11.6	8.7×10^{3}	2.3
	Cr2 state (TA 100°C)	3.6×10^{-2}		8.8×10^{4}	7.0
Ph-$(Tp)_3$-C12 [d]	Cr1 state (30°C)	3.9×10^{-3}	2.8	2.0×10^{4}	0.3
	Cr2 state (TA 90°C)	1.1×10^{-2}		3.0×10^{5}	2.2
Ph-$(Tp)_3$-C10	Cr1 state (30°C)	7.5×10^{-3}	2.0	1.4×10^{4}	0.9
	Cr2 state (TA 83°C)	1.5×10^{-2}		1.1×10^{5}	4.9
Ph-$(Tp)_3$-C8	Cr1 state (30°C)	2.0×10^{-3}	1.3	8.3×10^{3}	-2.7

	Cr1 state	(65°C)	2.5×10^{-3}		9.5×10^{3}	-4.1
Ph-$(Tp)_3$-C6	Cr1 state	(30°C)	1.4×10^{-3}	1.6	8.5×10^{2}	-5.0
	Cr1 state	(60°C)	2.2×10^{-3}		2.5×10^{3}	-4.8

a. Cr2 state was achieved by thermal annealing at certain temperatures in bracket for 5min and then cooling to 30°C;

b. all OFETs performance was obtained at V_{ds} = -50V, and the OFETs mobility was calculated from linear area of transfer characteristics;

c. mobility ratio of after and before TA.

d. the OFETs performance was optimized as Fig. 8a to set an optimized TA temperature at Cr2 state.

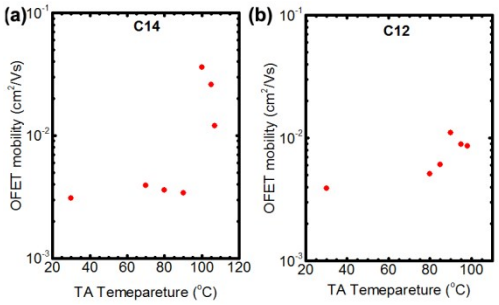

Fig. S8 FET mobility of as a function of TA temperatures in Cr state (a)Ph-$(Tp)_3$-C14 (b) Ph-$(Tp)_3$-C12